Effects of signaling on subcellular localization of MITF

Edda Sigrún Guðmundsdóttir

Effects of signaling on subcellular localization of MITF

Edda Sigrún Guðmundsdóttir

10 eininga ritgerð sem er hluti af
Baccalaureus Scientiarum gráðu í Sameindalíffræði

Leiðbeinendur
Eiríkur Steingrímsson
Valerie Fock

Effects of signaling on subcellular localization of MITF
10 eininga ritgerð sem er hluti af *Baccalaureus Scientiarum* gráðu í Sameindalíffræði

Útdráttur

Umritunarþátturinn MITF er þekktur fyrir að vera aðal stjórnþátturinn í litfrumum og spilar einnig stóran þátt í sortuæxlum. Vitað er að MITF er stjórnað af boðferlum, eins og MAPK boðferlinum en í honum er boðum miðlað með fosfórýlerun próteina. Dregið er úr virkni MAPK boðferilsins í að minnsta kosti 90% sortuæxla. Fosfórýlerun umritunarþátta getur haft áhrif á virkni þeirra, stöðugleika, prótein samskipti og innanfrumu staðsetningu þeirra. Ekki er mikið vitað um áhrif fosfórýlerunar á MITF en það er að jafnaði samþykkt að þegar serín set 73 og 409 eru fosfórýleruð hefur það áhrif á bæði umritunarvirkni og stöðugleika. Litrófsmælingar hafa gefið til kynna nokkur serín set í MITF sem eru fosfórýleruð en áhrif fosfórýleringarinnar hafa ekki verið rannsökuð. Markmið þessa verkefnis var að rannsaka hvernig mismunandi fosfórýleruð serín set hafa áhrif á staðsetningu MITF í frumu. Til að rannsaka þetta var notast við mismunandi serín set í MITF sem var áður búið að stökkbreyta í annaðhvort alanín (hindrar fosfórýlerun) eða glútamik sýru (líkir eftir fosfórýlerun). Í þessari rannsókn voru þessi stökkbreyttu MITF plasmíð sem jafnframt voru FLAG-merkt, yfirtjáð í mennsku sortuæxlisfrumulínunni Skmel28, en þessi frumulína ber BRAF stökkbreytingu (V600E) sem veldur ofvirkum MAPK boðferli. Mótefnalitun var svo framkvæmd og lagsjárskoðun notuð til að ákvarða staðsetningu stökkbreytts og venjulegs MITF innan frumu. Styrkleikamæling leiddi í ljós að stökkbreytingarnar S73A, S307A, S307E, S409A, S73/409A og S73/307A/409A höfðu allar áhrif á staðsetningu MITF innan frumu.

Abstract

Microphthalmia-associated transcription factor (MITF) is the master regulator of melanocytes and plays a crucial role in melanoma. MITF is known from the literature to be regulated by signaling, for example through the MAPK pathway which mediates signals with protein phosphorylations. The MAPK pathway is deregulated in at least 90% of all melanomas. When transcription factors are phosphorylated, it can affect their activity, stability, protein interactions and their subcellular localization. Not much is known about the effects of phosphorylation on MITF but it is generally accepted that when phosphorylated at serine sites 73 and 409, both its transcriptional activity and stability are affected. Mass spectrometry analysis has revealed several serine sites in MITF that are phosphorylated but the effects have not been investigated. The aim of this study was to investigate how various serine phosphorylations affect MITF's subcellular localization. To investigate this, various serine sites in MITF had previously been mutated to either alanine (inhibits phosphorylation) or glutamic acid (mimics the phosphorylated state). In this study, these mutant FLAG-tagged constructs were overexpressed in the human melanoma cell line Skmel28 carrying a BRAF mutation (V600E) and therefore exhibiting a hyperactive MAPK pathway. Immunostainings were then performed, and to determine the subcellular localization of the serine mutants to the wild type protein, confocal microscopy was used. Intensity quantifications revealed that the mutations S73A, S307A, S307E,

S409A, S73/409A and S73/307A/409A all affected the subcellular localization of MITF in terms of changes in nuclear and/or cytoplasmic staining intensity.

This thesis is dedicated to my best friend, Dagný Ösp and to my wonderful mother-in-law, Anna Guðrún, both of whom recently passed away.

Table of contents

Figures

Tables

Abbreviations

ATP	Adenosine triphosphate
bHLH-ZIP	Basic helic-loop-helix leucine zipper
BSA	Bovine serum albumin
cAMP	Cyclic adenosine monophospate
CBP	CREB binding protein
CREB	cAMP-response element binding protein
CSD	Chronically sun damaged
DAPI	4',6-diamidino-2-phenylindole
DMEM	Dulbecco's modified eagle medium
DNA	Deoxyribonucleic acid
ERK	Extracellular-regulated signal kinase
FCS	Fetal calf serum
GSK3(β)	Glycogen synthase kinase 3 (beta)
GTP	Guanosine triphosphate
JNK	Jun amino-terminal kinases
MAPK	Mitogen-activated protein kinase
MAPKK	Mitogen-activated protein kinase kinase
MAPKKK	Mitogen-activated protein kinase kinase kinase
MITF	Microphthalmia-associated transcription factor
NF	Neurofibromin
NGS	Normal goat serum
PBS	Phospate buffered saline
PFA	Paraformaldehyde

PKA	Protein kinase A
PTM	Post-translational modifications
rpm	Rounds per minute
RSK	Ribosomal S6 kinase
SAPK	Stress-activated protein kinase
SUMO	Small ubiquitin-related modifier
TYR	Tyrosinase
TYRP	Tyrosinase-related protein
UV	Ultra violet
WT	Wild type

Acknowledgements

1 Introduction

1.1 Melanocytes and melanoma

1.1.1 Melanocytes

Melanocytes are cells that produce the pigment melanin and can be found throughout the body, primarily in the epidermis and hair follicles. They are derived from the neural crest. Melanin plays an important role in the protection against solar UV radiation which causes DNA damage and is one of the major risk factors for skin cancer. Molecular recognition of melanocytes can be made using antibodies against the melanocyte-specific proteins tyrosinase (TYR), tyrosinase-related protein 1 and 2 (TYRP1, TYRP2/DCT), melanosomal matrix proteins (Pmel17, MART-1) and Microphthalmia-associated transcription factor (MITF). Mature melanocytes are either oval or fusiform in shape. They are dendritic cells and contain special membrane-bound organelles, called melanosomes, in their cytoplasm. Melanosomes are melanin-producing organelles and are transported to the dendrite tips of melanocytes and then to the surrounding keratinocytes. The association between these cell types also plays an important role in photoprotection of the skin cells (Cichorek et al., 2013).

1.1.2 Melanoma

A malignancy of the melanocytes is called melanoma. It is the most severe type of human skin cancer known and about 5 people die from it every year in Iceland (Landlæknisembættið, Hollráð). The most common treatment of melanocytes is a surgical removal of the melanoma. Unfortunately, melanomas are quite resistant to chemotherapy but recently novel therapeutics have been developed, both small molecules as well as immunotherapy.

Since melanocytes are derived from neural crest cells, melanomas can be found all over the body or where the melanocytes end up in development. The most common type of melanoma occurs in the epidermis, which gets exposed to ultra violet radiation from the sun. People with fair skin, freckles or red hair are more prone to developing skin cancer.

Melanomas that are found on sun-exposed skin can be divided into two groups: Chronically sun damaged (CSD) and non-CSD melanomas (Figure 1). These two subsets of melanoma differ from each other regarding the place of origin, time under UV radiation, age of the patient, mutations and oncogenic alterations (Shain & Bastian, 2016).

CSD melanomas occur on the skin of people older than 55 years of age that have been affected by a lot of UV radiation. These melanomas originate from sun-exposed areas such as the head and neck. The mutations present in these types of melanomas are commonly found within neurofibromin 1 (NF1), NRAS, BRAF (excluding the V600E mutation) or KIT. The proteins encoded by these genes form part of key signaling pathways that trigger proliferation.
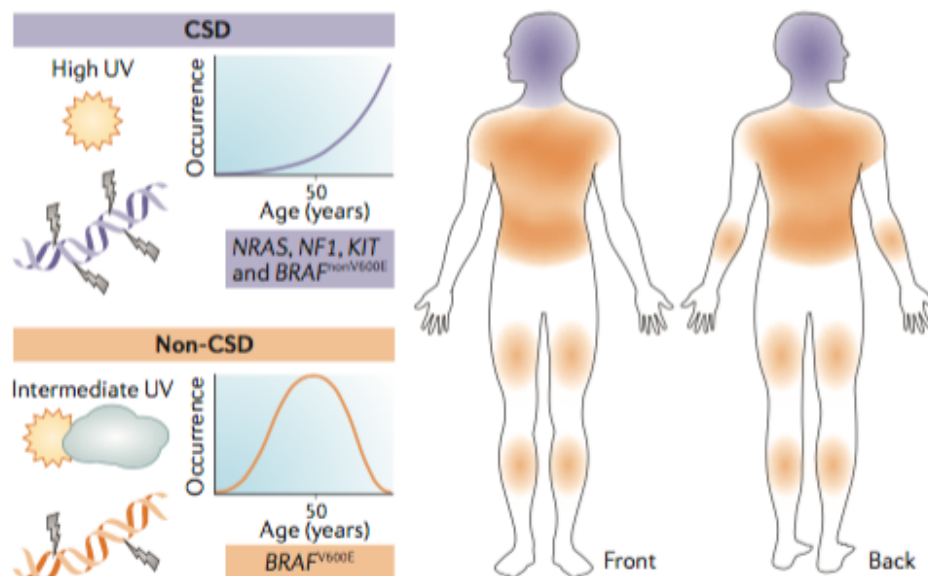
Figure 1: The difference between CSD and non-CSD melanomas. *The figure was taken from Shain & Bastian, 2016.*

Non-CSD melanomas occur in people younger than 55 years of age in areas that have not been exposed to UV radiation, such as the trunk. The characteristic of non-CSD melanomas is a mutation in BRAF, where a valine at position 600 is substituted with glutamic acid (V600E). This mimics the phosphorylated state of the protein and leads to hyper-activation of the mitogen-activated protein kinase pathway.

Melanomas can be easily detected because they are usually associated with naevi which are pigmented (Figure 2) and when melanogenesis starts, the pigment of the naevi changes (Shain & Bastian, 2016).
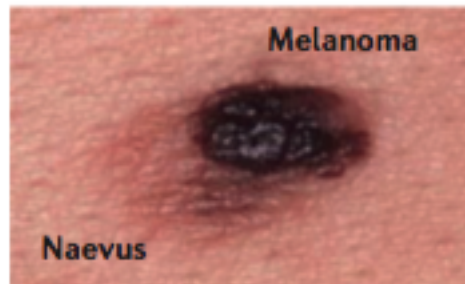
Figure 2: Melanoma in naevi. *This figure was taken from Shain & Bastian, 2016.*

1.2 MITF

Microphthalmia-associated transcription factor (MITF) is a basic helix-loop-helix leucine zipper (bHLH-ZIP) transcription factor (see Figure 3 for crystal structure). It regulates the expression of genes by binding to DNA response elements that contain E-box or M-box elements (CACGTG or CATGTG, respectively) (Wellbrock and Arozarena, 2015). MITF plays an important role in skin pigmentation, hearing and eye development. Many different isoforms of MITF are known and all of them are transcribed from the same MITF locus but different MITF promoters. All of the isoforms vary in the first exon. The first exon is spliced with exon 2 to exon 9 as those exons are conserved between all the isoforms. The transcript expressed in melanocytes, MITF-M, contains a short unique amino-end fused to the common exon 2. The different isoforms are responsible for the many tissue specific functions of MITF. They vary in molecular weight, ranging from 50 to 80 kDa.

1.2.1 MITF-M isoform

The MITF-M isoform is specifically expressed in the melanocyte lineage and its weight is around 50-65 kDa, making it the smallest MITF isoform known to date. Its expression is driven by the M-promoter of the MITF locus. MITF-M regulates melanoblast propagation in early development and melanogenesis in adult melanocytes. Its role is maintained in both melanocytes and melanomas.
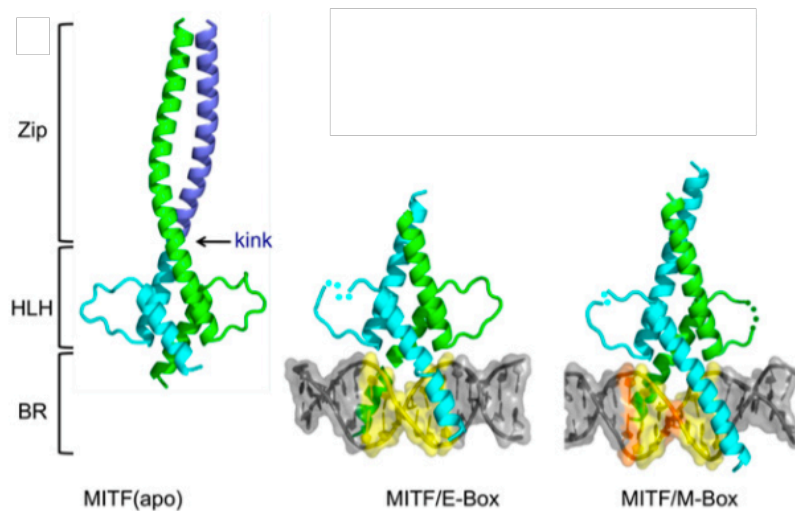
Figure 3: MITF crystal structures. *MITF (apo) is not bound to DNA. MITF/E-box or MITF/M-box shows MITF bound to either the E-box or the M-box on the DNA. Adapted from Pogenberg et al., 2012.*

1.2.2 MITF and its role in melanoma

The MITF-M isoform is expressed in more than 80% of all melanomas. MITF is known to be a lineage survival oncogene because it is required for proliferation and survival of melanoma cells. MITF is expressed throughout the entire tumor progression, allowing melanocytes to exit the cell cycle and differentiate, and therefore starting the melanogenesis program.

1.3 Signaling to MITF

MITF is known to be regulated through signaling pathways. For example, it has been shown that it is modulated by the MAPK pathway which affects both MITF activity and stability. Wnt signaling has been shown to affect MITF stability and the cyclic AMP pathway has been shown to regulate MITF expression.

The MAPK pathway affects MITF through phosphorylation by different MAP kinases such as extracellular-regulated signal kinase (ERK) and ribosomal S6 kinase (RSK). Here, phosphorylation of MITF has been shown to increase its activity, while simultaneously targeting the protein for proteasomal degradation (Wellbrock & Arozarena, 2015).

MITF has been shown to be located downstream of the Wnt pathway: in the presence of Wnt ligands, GSK3 becomes inactivated which in turn leads to MITF stabilization and target gene expression. Wnt signaling is frequently deregulated in cancer (Ploper et al., 2015).

The cAMP pathway affects MITF expression through cAMP-mediated PKA phosphorylation of CREB, which regulates various transcription factors that in turn activate MITF expression (Raker et al., 2016).

1.3.1 MAPK pathway

Mitogen-activated protein kinase (MAPK) modules contain three protein kinases that are activated sequentially (MAPKKK, MAPKK and MAPK). These kinases are important factors in signal transduction pathways that regulate cell proliferation, cell differentiation and cell survival. Extracellular signals such as growth factors or cytokines bound to a cell surface receptor activate MAPKKK through phosphorylation by protein kinases downstream of the receptor and/or interactions with a small GTPase. Activated MAPKKK directly phosphorylates and therefore activates MAPKK that activates MAPK again via phosphorylation. Activated MAPK phosphorylates its substrates in the cytoplasm and/or nucleus. The consequences are changes in protein function and gene expression that lead to a biological response. The MAPKs in mammals can be grouped into three main families, as shown in Figure 4: extracellular-signal-regulated kinases (ERKs), Jun amino-terminal kinases (JNKs) and p38/stress-activated protein kinase (SAPKs) (Morrison, 2012).
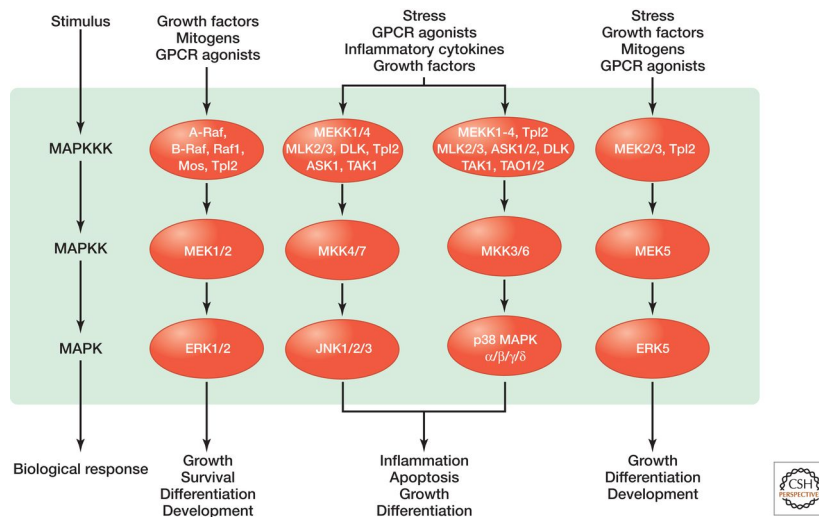
Figure 4: The MAP kinase pathway. *Shown are the three main pathways mediating signals via ERK, JNK and p38, resulting in diverse biological responses such as growth, survival, differentiation or cell death.*

1.3.2 Wnt pathway

Cell transformation and differentiation are in some cases based on the activation of the Wnt pathway that involves the multifunctional protein β-catenin.

Wnt proteins act as short or long range signaling molecules that bind to transmembrane receptors of the Frizzled family and several co-receptors. When Wnt proteins bind to Frizzled receptors, they trigger a cellular response to activate intracellular signaling pathways that induce gene expression (Rao and Kühl. 2010).

When Wnt ligands bind to their receptors (Frizzled), they prompt the Dishevelled protein, which is a cytoplasmic phospho-protein downstream of the Frizzled receptor, to prevent the destruction of β-catenin because GSK3β-mediated phosphorylation triggers β-catenin degradation. β-catenin then moves to the nucleus and converts the T cell factors, that act as transcriptional repressors, into transcriptional activators. Glycogen synthase kinase 3 beta (GSK3β) is known from the literature to mediate the relationship between Wnt signaling and β-catenin transcriptional activity (Bowerman, 2008).

1.3.3 cAMP pathway

Cyclic adenosine monophospate (cAMP) is known to be an intracellular second messenger of extracellular ligand action. It regulates metabolism and gene expression. cAMP is

6

formed from ATP and enzymes of the adenylate cyclases (AC) family catalyze this reaction (Raker et al., 2016).

cAMP activates cAMP-dependent protein kinase A (PKA). When cAMP binds to its regulatory subunits, PKA splits into its subunits. These catalytic subunits of PKA phosphorylate specific Thr and Ser sites on many target proteins. cAMP-response element binding protein (CREB) is a cAMP-responsive transcription factor that cAMP-activated PKA binds to and phosphorylates. CREB then binds to the cAMP response element TGACGTCA (Delghandi et al., 2005) which is usually found in the promoter of cAMP-responsive genes.

1.3.4 Pathway activity in melanomas

The MAPK pathway is deregulated in more than 90% of melanomas. Melanoma cells frequently carry a BRAF mutation (V600E) which in turn makes the MAPK pathway hyperactive. MITF expression is then driven constitutively leading to cell survival and proliferation of melanoma cells.

It has been shown that the cAMP pathway is preserved throughout melanoma progression which keeps MITF transcribed throughout melanogenesis. SOX10 is a transcription factor that binds to the MITF promoter (Bondurand et al., 2000; Lee et al., 2000; Potterf et al., 2000; Verastegui et al., 2000) and is crucial for melanoma cell survival. SOX10 associates with CREB to increase MITF expression.

When β-catenin is overexpressed, it is not degraded by phosphorylation signals from GSK3 and as a consequence it is able to stimulate melanoma cell growth through MITF overexpression.

1.4 Post-translational modifications

Post-translational modifications (PTM) are chemical modifications of a protein that can happen throughout the "life cycle" of a protein. PTM can affect the function of a protein. MITF has been described to be a target of the following PTMs ("Overview of Post-Translational Modifications", year unknown):

1.4.1 Ubiquitination

Ubiquitin is a protein that covalently attaches to its target protein through the amino group of a lysine side chain. The most common form of ubiquitination is when an ubiquitin chain is formed, called polyubiquitin. A new ubiquitin links to Lys48 of the attached ubiquitin and so forth, forming the polyubiquitin. The most common effect on the protein when ubiquinated is that the protein is directed to the proteosome where it finally becomes degraded (Alberts et al., 2015).

1.4.2 Sumoylation

Small ubiquitin-related modifier (SUMO) is a protein that belongs to the ubiquitin family and acts similar to ubiquitination. SUMO also covalently binds to a lysine side chain of the target protein (Alberts et al., 2015). When proteins are modified with SUMO, it can affect their protein-protein interactions, localization, activity or degradation.

1.4.3 Acetylation

When acetyl groups are added to specific lysine sites on the N-terminal end of histone tails, it loosens the chromatin structure and can stimulate transcription initiation. Histone acetylation therefore always correlates with gene activation (Alberts et al., 2015). Acetylation of transcription factors has started to appear as an important modification of their activity.

1.4.4 Phosphorylation

The most common way of regulating the function of a protein is the addition of a phosphate group to a protein. A protein kinase is the key player in the addition of phosphate groups. It catalyzes the cleavage reaction of the terminal phosphate group of ATP (which acts as a co-substrate for almost all protein kinases) and transfers it to serine, threonine or tyrosine sites of the target protein. Phosphorylation plays an important role in the regulation of many cellular processes, including proliferation, cell function and signal transduction pathways. Since this particular PTM is reversible, it makes protein phosphorylation ideal for signal transduction pathways, therefore allowing the cell to respond to intra- or extracellular stimuli.

Phosphorylation of transcription factors can affect their activity, target gene expression, stability, degradation, interactions with other factors and their subcellular localization (Alberts et al., 2015).

To study phosphorylation effects, the phosphorylation sites of a protein can be mutated to a different kind of amino acid, such as alanine, that cannot be phosphorylated. Phosphorylation sites can also be mutated to amino acids that mimic the phosphorylated state of a protein, like glutamic acid or aspartic acid. These amino acids are chemically similar to phosphorylated amino acids and the protein maintains its level of activity or in some cases such changes can even increase protein activity.

Mass spectrometry analysis is often used to recognize unknown phosphorylation sites of a protein. Stable isotope labeling by amino acids in cell culture or labeling of peptides with tandem mass tags are then used for determination of changes in phosphorylation states ("Phosphorylation", year unknown).

1.5 MITF and its post-translational modifications

Phosphorylation of MITF by MAPK, RSK, GSK3β and p38 are well described PTMs, which have been shown to affect activity, stability and target gene repertoire of the protein, resulting in changes in cellular processes.

Downstream of the receptor tyrosine kinase KIT is the MAP kinase ERK that phosphorylates MITF at its serine residue S73 (Figure 5). When S73 is phosphorylated, an increase in the interaction between PIAS3 and MITF takes place, which represses MITF transcriptional activity.
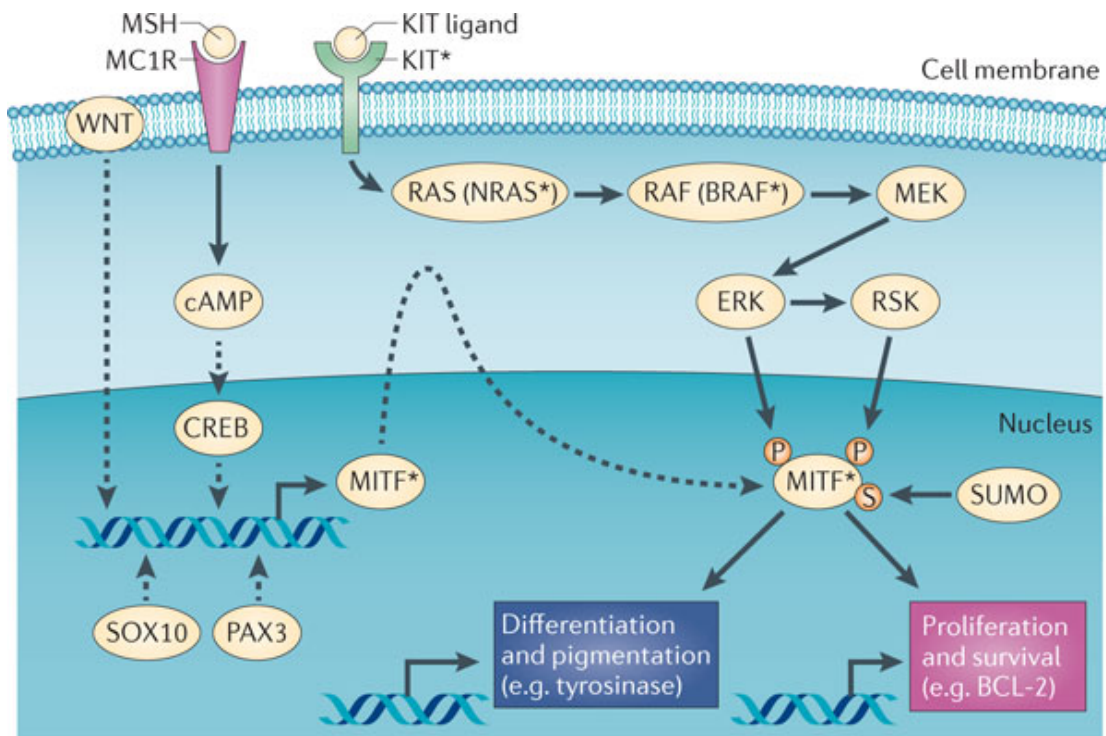
Figure 5: Signaling pathways affecting MITF. This figure shows WNT, cAMP and MAPK pathways.

If this phosphorylation occurs when BRAF carries a hyperactive mutation (V600E), MITF's transcription activity is enhanced at the *Tyrosinase* promoter through increased interactions with the acetyltransferase of p300/CREB binding protein (CBP) in melanoma cells (Price et al., 1998).

When S73 is mutated to alanine, the site can not be phosphorylated and MITF's transcription activity is impaired (Wellbrock & Arozarena, 2015).

ERK activates RSK by phosphorylation and RSK in turn phosphorylates MITF at S409, when KIT ligand is bound to KIT receptor. When S409 is phosphorylated, it acts as a priming site for GSK3. Proteins phosphorylated by GSK3 are generally targeted for degradation. Phosphorylated MITF at S409 would therefore be expected to have reduced transcription activity. It has been shown, however, that when S409 is mutated to alanine, it has no striking effect on MITF's transactivation of the *Tyrosinase* promoter. When the S73A/S409A double mutant was generated it appeared to suppress transcription from the Tyrosinase promoter. As a consequence this double mutant results in a protein that is somewhat stable and transcriptionally inactive. Phosphorylations of S73 and S409 are required for proteasome-mediated degradation.

10

Phosphorylation of MITF by GSK3β has been at S397, S401 and S405 and shown to affect MITF degradation/stability. Accordingly, when these sites are mutated to alanines it enhances the stability of MITF (Ploper et al., 2015).

According to recent mass spectrometry analysis performed by our laboratory, the serine sites 100, 307 and 384 of wild type MITF also appear to be phosphorylated. While no information regarding kinases targeting these sites exists for S100 and S384, S307 is known to be phosphorylated by p38 in osteoclasts (Mansky et al, 2002).

2 Aim of this project

Phosphorylation of transcription factors in response to signaling pathways can affect these proteins in several ways, such as influencing their activity, interactions with other proteins, stability or subcellular localization. In regard to MITF-M, which is mainly located within the nucleus of melanoma cells, not much is known about how phosphorylation of different serine sites affects its subcellular localization. To address this question, different serine sites of MITF-M have been previously mutated to alanine (S-to-A) or glutamic acid (S-to-E) in a FLAG vector backbone to determine the effects on the subcellular localization of MITF-M. In this project, these constructs were overexpressed in Skmel28 melanoma cells, followed by immunostainings, and confocal microscopy. Intensity quantifications were then performed to thoroughly analyze the localization pattern of the diverse MITF mutants compared to the wild type protein.

3 Materials and methods

3.1 List of plasmids

Table 1: List of plasmids. *This table shows the names of each plasmid that was used, its backbone, resistance and it's owner/creator.*

Name	Vector backbone	Resistance	Made by/received from
mMITF +18 WT	p3XFLAG-CMV™-14	Amp^R	Jane Goodall
mMITF +18 S73A	p3XFLAG-CMV™-14	Amp^R	Josue Ballesteros
mMITF +18 S409A	p3XFLAG-CMV™-14	Amp^R	Josue Ballesteros
mMITF +18 S73/409A	p3XFLAG-CMV™-14	Amp^R	Josue Ballesteros
mMITF +18 S307A	p3XFLAG-CMV™-14	Amp^R	Alexander Schepsky
mMITF +18 S307E	p3XFLAG-CMV™-14	Amp^R	Alexander Schepsky
mMITF +18 S100A	p3XFLAG-CMV™-14	Amp^R	Bengt Phung
mMITF +18 S298A	p3XFLAG-CMV™-14	Amp^R	Bengt Phung
mMITF +18 S384A	p3XFLAG-CMV™-14	Amp^R	Bengt Phung
mMITF +18 S397A	p3XFLAG-CMV™-14	Amp^R	Bengt Phung
mMITF +18 S298/307/384A	p3XFLAG-CMV™-14	Amp^R	Bengt Phung
mMITF +18 S298/384/397A	p3XFLAG-CMV™-14	Amp^R	Bengt Phung
mMITF +18	p3XFLAG-CMV™-15	Amp^R	Alexander Schepsky

S73/307/409A			

3.2 DNA concentration measurements

Plasmid DNA concentration was determined by using NanoDrop (ND-1000) The DNA-50 program was used. The surface was cleaned thoroughly with a tissue and then the blank was prepared with 2 µL of H_2O. The water was wiped off and finally 2 µL of plasmid DNA were put on top and its concentration was measured. The results were given in ng/µL.

3.3 Transformation of E.coli strain DH5-α

5 ng plasmid DNA were needed for the transformation of bacteria and the volume for each plasmid was calculated as follows (concentration of wild type MITF plasmid with a concentration of 102.4 ng/L is used as an example):

$$5 \text{ ng} * 1 \text{ µL} \div 102.4 \text{ ng} = 0{,}05 \text{ µL DNA}$$

The DNA was diluted with 100 µL of dH_2O so the final volume would be manageable to pipette:

$$5 \text{ ng} * 100 \text{ µL} \div 102.4 \text{ ng} = 5 \text{ µL}$$

E.coli were taken up from the −80°C freezer and carefully thawed on ice. 100 µL of E.coli cells per reaction were pipetted into a 1.5 mL Eppendorf tube that was kept on ice. The exact volume needed for getting 5 ng of plasmid DNA was added to the E.coli cells with a pipette. Bacteria and DNA were carefully mixed together by flicking the tube four to five times. After addition of DNA, the mixture was kept on ice for 30 minutes followed by a heat shock in a water bath at exactly 42°C for 30 seconds. Immediately after the heat shock, bacteria were placed on ice for 5 minutes after which 950 µL of LB medium were added to the mixture. The mixture was then placed into a shaker (Eppendorf, Thermomixer compact) and incubated at 250 rpm for 1 hour at 37°C. In the meantime, ampicillin-containing agar plates were warmed up to 37°C. After the incubation, 90 µL and 150 µL

were spread on separate agar plates, incubated overnight at 37°C and afterwards put into the cold room to slow down cell growth.

3.4 DNA purification (Midiprep)

The GeneJet Plasmid MidiPrep Kit was used for this procedure (Thermo Scientific).

For preparing a starter culture, 3 mL of LB medium were added together with 6 µL of ampicillin (1:500) into a falcon tube. One colony was picked with a yellow pipette tip from an agar plate for each plasmid and added into individual Falcon tubes, which were then incubated in a bacteria shaker (New Brunswick Scientific, C25 incubator shaker) at 230 rpm and 37°C for 5 hours.

Subsequently, the Falcon tubes were removed from the incubator and for each plasmid a glycerol stock was prepared by adding 500 µL glycerol (Sigma-Aldrich) and 500 µL of amplified bacteria into an Eppendorf tube, which was then stored at -80°C.

For overnight cultures, 50 mL LB medium and 50 µL ampicillin (1:1000) were added together into 250 mL Erlenmeyer flasks. 100 µL of amplified bacteria were carefully pipetted into the growth medium and incubated in a bacteria shaker at 230 rpm and 37°C for 18 hours. After overnight incubation, bacteria were transferred into a 50 mL falcon tube and the cells were harvested by centrifuging for 10 minutes at 4700 rpm (Thermo Scientific, Heraeus Multifuge X3R). After discarding the supernatant, 2 mL of Resuspension Solution (supplemented with RNase A Solution) was added to the pelleted cells, which were resuspended by vortexing until no cell clumps were visible within the solution. 2 mL of Lysis Solution were then carefully added to the cell suspension by inverting the tube 5 times, followed by incubation at room temperature for 3 minutes. Subsequently, 2 mL of Neutralization Solution were mixed immediately with the solution by inverting the tube 6 times. 0.5 mL of Endotoxin Binding Reagent were added to the mixture and the tube was inverted as before. The suspension was incubated at room temperature for 5 minutes, followed by the addition of 3 mL 96% ethanol. After inverting the tubes, the mixture was centrifuged for 40 minutes at 4700 rpm to pellet chromosomal DNA and cell debris.

After centrifugation, the supernatant was carefully pipetted into a 15 mL Falcon tube, without transferring the white precipitate containing cell debris and chromosomal DNA. 3

mL of 96% ethanol were added as before. 5.5 mL of the solution were transferred into a supplied column, which was placed into a 15 mL collection tube. The tubes were then centrifuged for 3 minutes at 2000 rpm. The flow through was discarded and the remaining supernatant was added to the same column, followed by another centrifugation step.

4 mL of Wash Solution I (diluted with isopropanol) were added to the column after both centrifugations. The column was centrifuged at 3000 rpm for 2 minutes and the flow through was discarded. 4 mL of Wash Solution II (diluted with ethanol) were added to the column and centrifuged for another 2 minutes at 3000 rpm. The flow through was again discarded. This step was repeated with Wash Solution II.

The column was again centrifuged for 5 minutes at 3000 rpm in order to remove any residual wash solution. The flow through was discarded from the collection tube. The column was then transferred into a new and clean 15 mL collection tube. 0.35 mL of Elution Buffer were added to the center of the column membrane and incubated at room temperature for 2 minutes. After that time, it was centrifuged for 5 minutes at 3000 rpm to elute the plasmid DNA that was bound to the purification column.

The plasmid DNA was transferred into a 1.5 mL Eppendorf tube and the DNA concentration was measured using NanoDrop. Finally, DNA was stored at -20°C.

3.5 Cell culture

The human melanoma cell line Skmel28 was retrieved from the liquid nitrogen tank and thawed until no crystals remained. After centrifuging for 3 minutes at 2000 rpm, cells were resuspended in Dulbecco's Modified Eagle Medium (DMEM; 4.5 g/L D-Glucose, Pyruvate) which was supplemented with 10% fetal calf serum (FCS), by adding 50 mL FCS to 450 mL DMEM. Skmel28 cells were pipetted onto a 10 cm culture plate. The cells were incubated at 37°C with 5% CO_2 for 3 to 5 days or until they had reached ~80% confluency.

3.5.1 Splitting cells

When the cells had reached confluency, the medium was removed and 5 mL phosphate-buffered saline (PBS) were added to the edge of the plate, which was then slowly moved in a circular motion to carefully wash the cells. After removing the PBS, 1 mL Trypsin

(Gibco) was added to the plate and incubated for 2-3 minutes to detach the cells from the culture plate as well as to loosen cell-cell contacts. The trypsin was deactivated with 5 mL of culture medium (DMEM+FCS). The cell suspension was then taken up using a pipette and transferred into a 15 mL Falcon tube. The cells were centrifuged for 3 minutes at 2000 rpm. The supernatant was discarded and the cell pellet was resuspended in 1 mL culture medium by pipetting up and down and then 4 mL medium were added on top. The cells were split in a 1:5 or 1:10 ratio onto new culture plates and cultivated in 10 mL medium as described above.

3.5.2 Seeding cells for transient transfections

After obtaining a single cell suspension, 10 µL were taken out of the cell solution and added under a cover slip, which was placed on top of a cell counter glass slide (Neubauer Improved). The counting chamber was then analyzed on a microscope (Olympus CKX41) and counted manually by using a manual counter tool. Four squares composed of 16 smaller squares were observable in the microscope. Only cells within those four squares were counted and the amount of cells in 1 mL was determined using the following equation:

Average of cells in four squares * 10.000 = cells per 1 mL

Cells were seeded onto 8-well chamber slides (Sigma-Aldrich, Nunc Lab-Tek® II) for transfection. 15.000 cells was the recommended amount to seed into each well in a final volume of 250 µL. To find the volume of cell solution the following equation was used:

15.000 cells per well ÷ cells per 1 mL = mL of cell solution per well

The volume of cell suspension needed for one well was multiplied by 9, because with 8 wells per slide, the total amount was accounted for 9 wells in consideration of possible pipetting errors.

In each well the total volume was supposed to be 250 µL.

9 wells * 250 µL = 2250 µL

The 9x cell solution was subtracted from the total volume, in this case 2250 µL, to get the final volume of medium to add into the mixture:

$$2250\ \mu L - 9x\ \mu L = \text{volume of medium in } \mu L$$

Finally, a cell suspension containing 135.000 cells in 2,25 mL was prepared and 250 μL (containing 15.000 cells) were pipetted into each well. The chamber slide was incubated overnight at 37°C and 5% CO_2.

3.5.3 Transient transfections

A transfection protocol from the online FuGene Database was obtained by filling in information about the cell line, what kind of plate would be used and number of wells being transfected. A total of 12 μL of plasmid solution and medium (DMEM without FCS) were prepared. First, the volume for 0.25 μg of DNA was calculated:

ng/μL DNA converted to μg/μL $\rightarrow$ Multiply by 1000
0.25 μg ÷ (μg/μL DNA) = μL of DNA required

The DNA volume was subtracted from 12 μL (total volume) to achieve the volume of DMEM. DNA and DMEM were mixed together into a small tube (Sarstedt 0.2 mL PCR tube). FuGENE® HD reagent was vortexed before adding 0.7 μL into the DNA mixture. The tube containing the transfection mix was carefully flicked 5 times followed by incubation at room temperature for 5-10 minutes. After incubation, 11 μL of the mixture were added into each well, the first well served as non-transfected control. The chamber slide was then incubated for 24 hours at 37°C.

3.6 Immunofluorescence stainings and confocal microscopy

3.6.1 Fixing cells

After incubation for one day, the transfected cells on the chamber slide were fixed. Therefore, 4% paraformaldehyde (PFA) was prepared by diluting 1 mL of 16% PFA (Thermo Scientific) with 3 mL of PBS. Liquid was aspirated from the chamber slide and the cells were rinsed with PBS 3 times. 250 μL of 4% PFA were then added into each well and the cells were fixed for 10 minutes at room temperature. Subsequently, the fixative was removed and the cells were rinsed 3 times with PBS. The slide was kept in PBS at 4°C until the immunostainings were performed.

3.6.2 Immunostaining

Immunostainings were carried out according to the Cell Signaling Technology protocol. At first, blocking buffer and antibody dilution buffer were prepared as follows: 10 mL of blocking buffer was prepared by adding 0.5 mL of Normal Goat Serum (NGS, Gibco) into 9 mL 1X PBS. After mixing, 30 μL of Triton™ X-100 (Merck) were added to the mixture. Blocking buffer is used to reduce non-specific antibody binding.

10 mL of antibody dilution buffer were prepared by mixing together 10 mL 1X PBS, 30 μL of Triton™ X-100 and 0.1 g of bovine serum albumin (Sigma-Aldrich).

The remaining PBS was removed from the fixed chamber slide. The cells were incubated in blocking buffer for 1 hour. In the meantime, a primary antibody solution was prepared by adding mouse monoclonal anti-FLAG® M2 antibody (Sigma-Aldrich) into antibody dilution buffer in a 1:5000 ratio. The blocking buffer was aspirated from the chamber slide and 200 μL of primary antibody solution was added to each well. The chamber slide was then incubated overnight at 4°C.

After overnight incubation, a fluorochrome-conjugated secondary antibody dilution was prepared by adding Alexa Fluor 546 anti-mouse IgG (Life Technologies) 1:1000 into antibody dilution buffer. DAPI was added in a 1:5000 dilution (Thermo Fisher Scientific). DAPI stains nuclei and the fluorochrome-conjugated secondary antibody detects the primary antibody that is bound to FLAG-tagged MITF. The secondary antibody illuminates under fluorescence light.

The diluted primary antibody was aspirated from the cells and they were rinsed three times with PBS. 200 μL of the fluorochrome-conjugated secondary antibody + DAPI solution was added into each well and incubated for 1 hour at room temperature in the dark (to prevent fluorochrome bleaching). After the incubation period, the solution was removed and the cells were rinsed three times with PBS. After rinsing, the chamber itself was removed from the slide. After removing all excess liquid, one drop of FluoroShield (Sigma-Aldrich) was added onto every other well and a cover slip was put on top. If bubbles formed, they were removed by pushing them to the edges of the cover slip with a yellow pipette tip. The cover slip was then glued onto the slide by applying Fixogum

(Marabu) around the edges of the cover slip. Each slide was kept in a light-isolating box at 4°C until further analysis using confocal microscopy.

3.6.3 Confocal microscopy

After the slides were prepared, they were taken to the confocal microscope (Olympus IX83) to visualize FLAG-tagged MITF constructs. The software was programmed to match the antibodies used. Pictures were taken using two lasers, the 405 (detecting DAPI) and the 543 laser (detecting red). The nucleus illuminated in blue and the MITF FLAG-tagged protein illuminated in red. Pictures were taken at a 60x lense with a resolution of either 1024*1024 pixels or 2048*2048 pixels.

3.7 Scoring

For each construct, approximately three images showing 2 stained cells were taken and with a total of 4 repeats, around twelve images per construct were used for analysis. To determine the nuclear and cytoplasmic staining intensity for each construct, three spots in each cell's nucleus and cytoplasm were quantified by using ImageJ and then the average was calculated for both the nuclear and cytoplasmic mean intensity values. To correct for the background, three spots in the background were quantified for each image. The averaged nuclear and cytoplasmic values for each construct were then divided by the averaged background values to obtain adjusted mean intensities.

Standard deviations were calculated from the raw values for every construct and then a student's T-test was performed to determine whether a specific serine mutant construct showed a significant difference in nuclear and/or cytoplasmic staining intensities compared to the wild type construct. If the p value was less than 0.05, the results were considered as statistically significant (marked with the symbol *). The results were then displayed using a column chart.

After each construct had been quantified, the mean intensity was further expressed in percentages. Here, the total MITF staining intensity (both nucleus and cytoplasm) was set to 100%. This was achieved by dividing the raw value for each construct's cytoplasm or nucleus with the total intensity of the cytoplasm and nucleus. The results were then multiplied with 100 to get the values in percentages. The standard deviation was calculated for each construct and the results were displayed with a column chart.

4 Results

In order to analyze the effects of serine phosphorylations on MITF's subcellular localization, various serine-to-alanine or serine-to-glutamic acid mutations were previously introduced in MITF (constructs are listed in Table 1 in the materials and methods chapter). The serine sites in focus are shown in Figure 6, and besides single mutants, double and triple mutations were introduced.
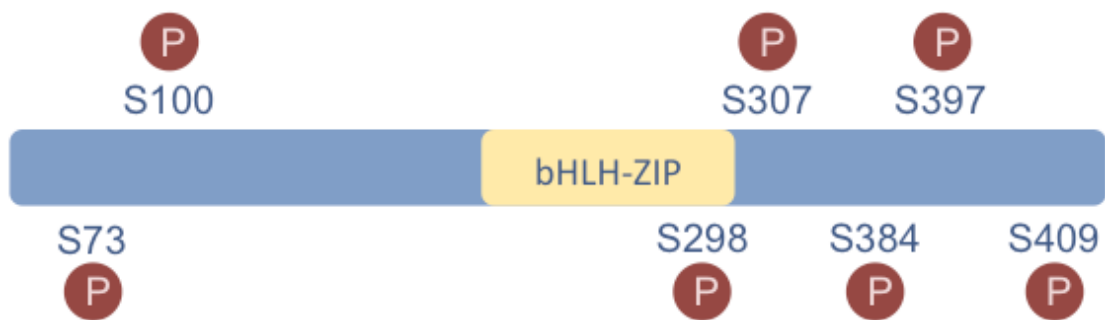

Figure 6: Serine sites on MITF. *These sites were shown to be phosphorylated by recent studies or mass spectrometry analysis. These sites were mutated and the effect on MITF's subcellular localization was assessed.*

The serine mutant constructs were overexpressed in Skmel28 cells, a human melanoma cell line carrying the V600E BRAF mutation. In order to visualize the constructs, anti-FLAG and DAPI stainings were performed. The following confocal images show anti-FLAG staining on the left and merged anti-FLAG and DAPI staining on the right.

Figure 7 shows the subcellular localization of wild type MITF. The MITF signal is mostly nuclear, but there is a weak signal visible in the cytoplasm.
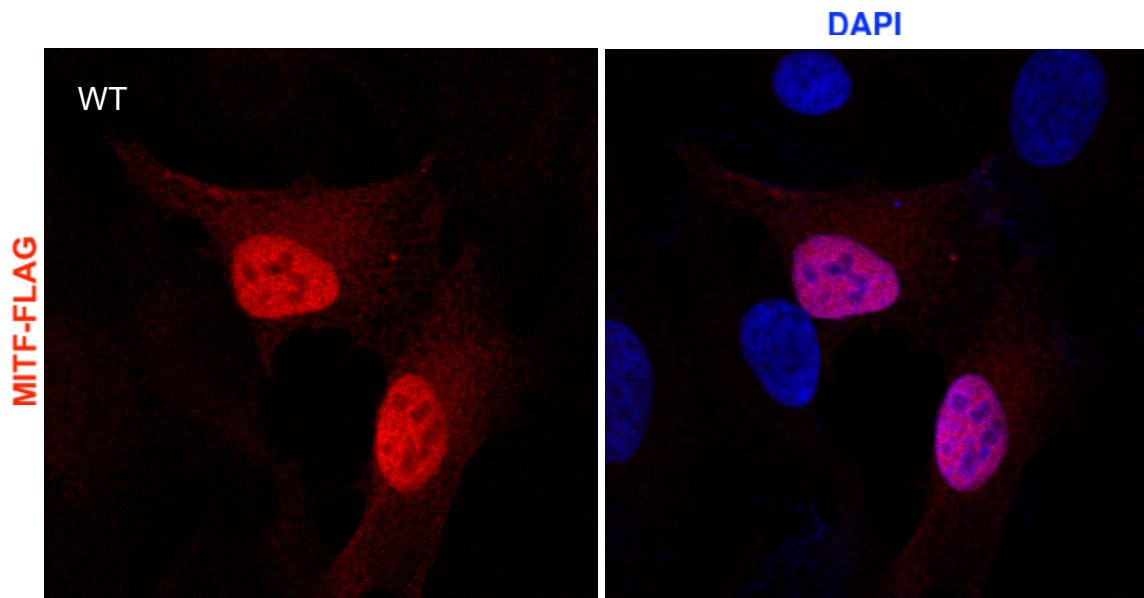
Figure 7: Representative confocal image of wild type MITF overexpressed in Skmel28 cells. *MITF is mostly nuclear but a minor fraction is also localized within the cytoplasm.*

4.1 Constructs having significant effects on subcellular localization of MITF

Representative images were chosen for each of the following serine mutant constructs (Figures 7-12). Figures 7-12 show constructs having significant effects on the subcellular localization of MITF compared to the wild type construct (shown in Figure 7). In order to determine statistical significance, staining intensity levels were quantified for each construct in the nucleus and cytoplasm using the ImageJ software. About 22 cells per construct were evaluated. The results for each construct were then compared to the wild type by using Student's unpaired T-test. The results are shown in Figures 14 and 15.
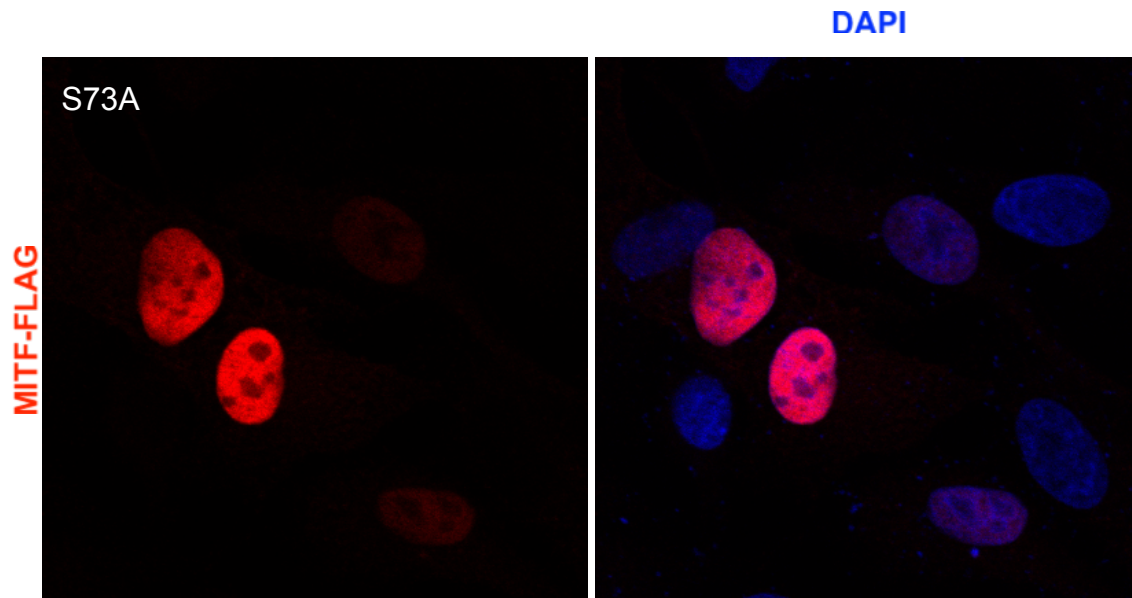
Figure 8: Representative confocal image of the S73A construct overexpressed in Skmel28 cells. *MITF is only visible in the nucleus.*
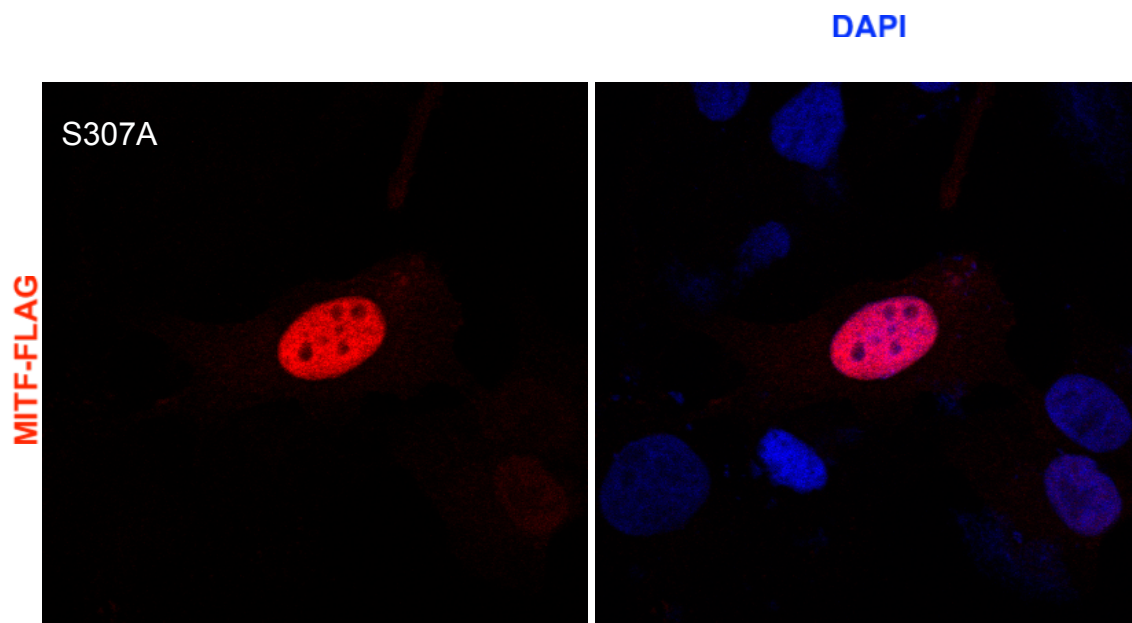

Figure 9: Representative confocal image of the S307A mutant construct overexpressed in Skmel28 cells. *MITF is mostly nuclear although there is a very weak signal noticable in the cytoplasm.*

Figures 8 and 9 show images of S73A and S307A mutant constructs. A strong nuclear signal is visible in the nucleus of both of the constructs. While no signal can be observed in the cytoplasm of S73A, a very weak signal can be seen in the cytoplasm of the S307A mutant construct.
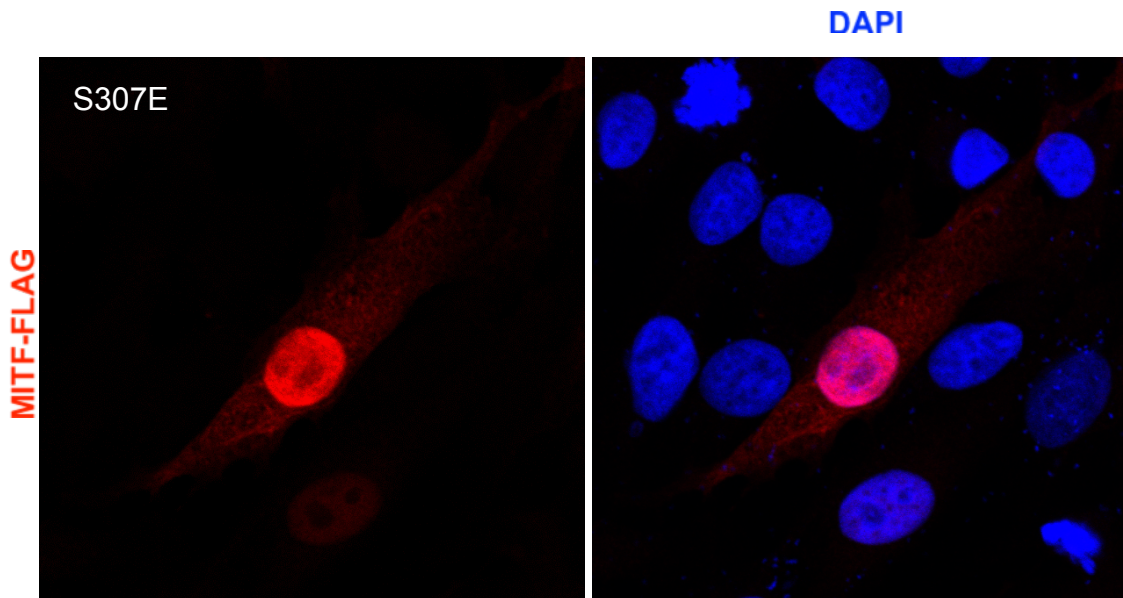
Figure 10: Representative confocal image of the S307E mutant construct overexpressed in Skmel28 cells. *This construct is very similar to the wild type construct: mostly nuclear with a weak signal in the cytoplasm.*
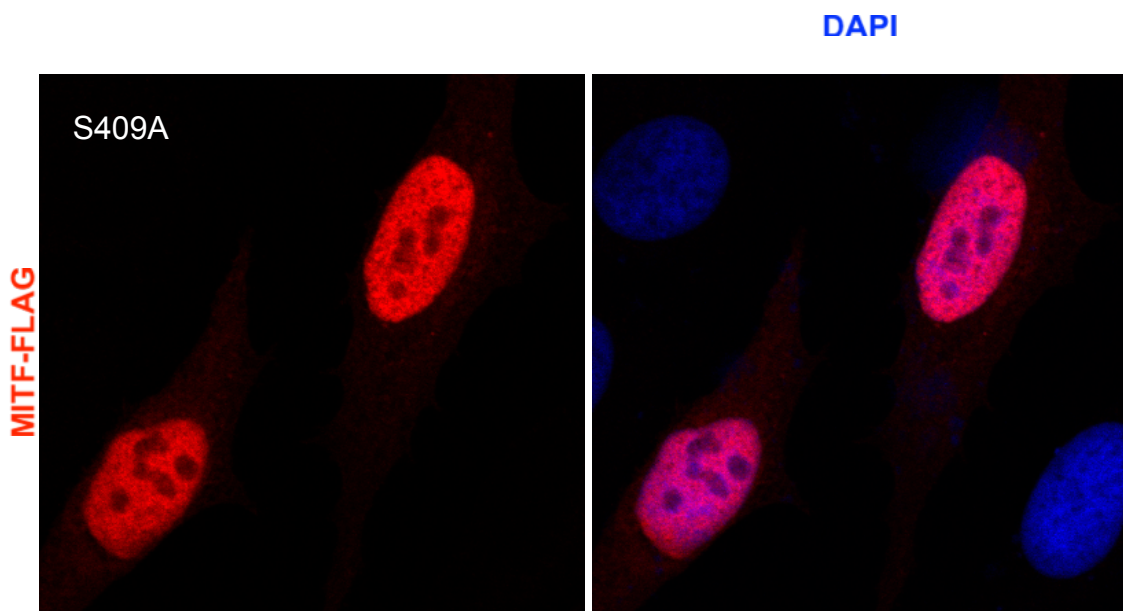

Figure 11: Representative confocal image of the S409A mutant construct overexpressed in Skmel28 cells. *This mutant shows a very strong nuclear signal and weak cytoplasmic signal.*

Figure 10 shows the staining pattern of the S307E mutant construct. Here, serine was mutated to glutamic acid, which is an amino acid residue used to mimic the phosphorylated state of a protein The construct is very similar to the wild type construct, showing a strong nuclear and a weak cytoplasmic signal.

24

The mutant construct S409A (Figure 11) shows a strong nuclear staining. A weak cytoplasmic signal is also visible.
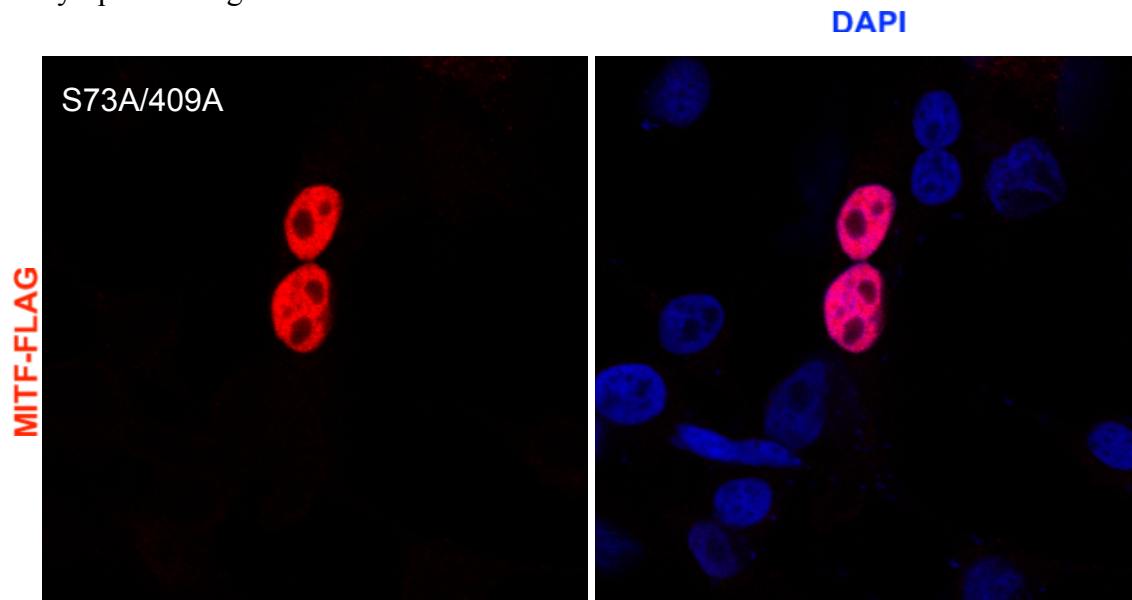

Figure 12: Representative confocal image of the S73A/S409A mutant construct overexpressed in Skmel28 cells. *A strong nuclear staining is visible, whereas no cytoplasmic staining can be observed.*

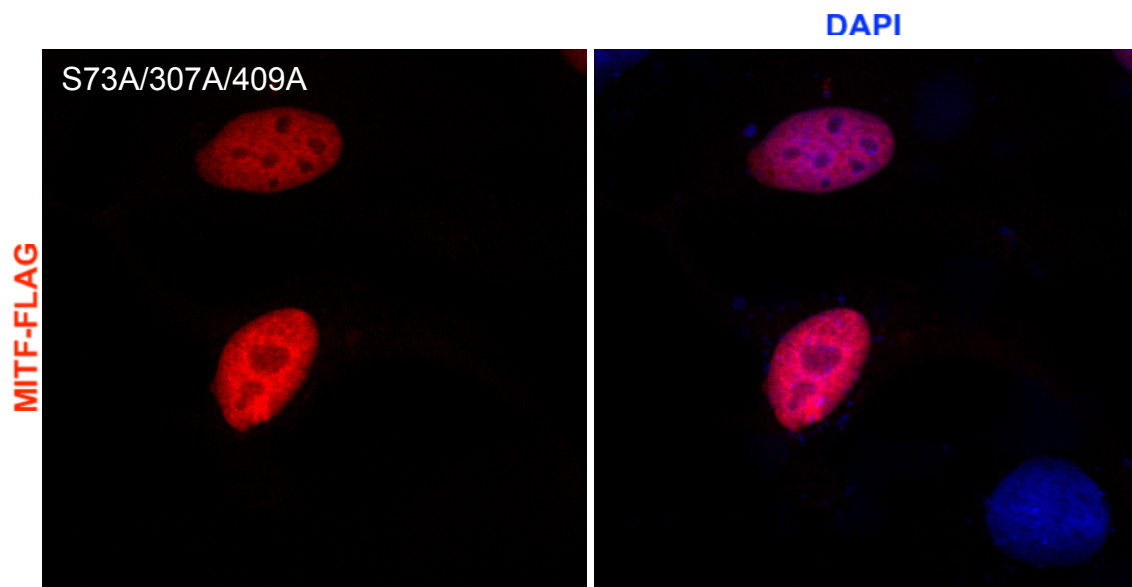**Figure 13: Representative confocal image of the S73A/307A/409A triple mutant construct overexpressed in Skmel28 cells.** *Only nuclear staining is visible. The construct shows a very similar pattern to the mutant constructs S73A and S73A/S409A.*

Figures 12 and 13 show double and triple mutant constructs, both containing the S73A and S409A mutations. The triple mutant additionally contains a S307A mutation. Both of these

constructs show no cytoplasmic staining but the double mutant (Figure 12) shows a stronger nuclear signal than the triple mutant (Figure 13).

4.1.1 Mean intensity quantifications
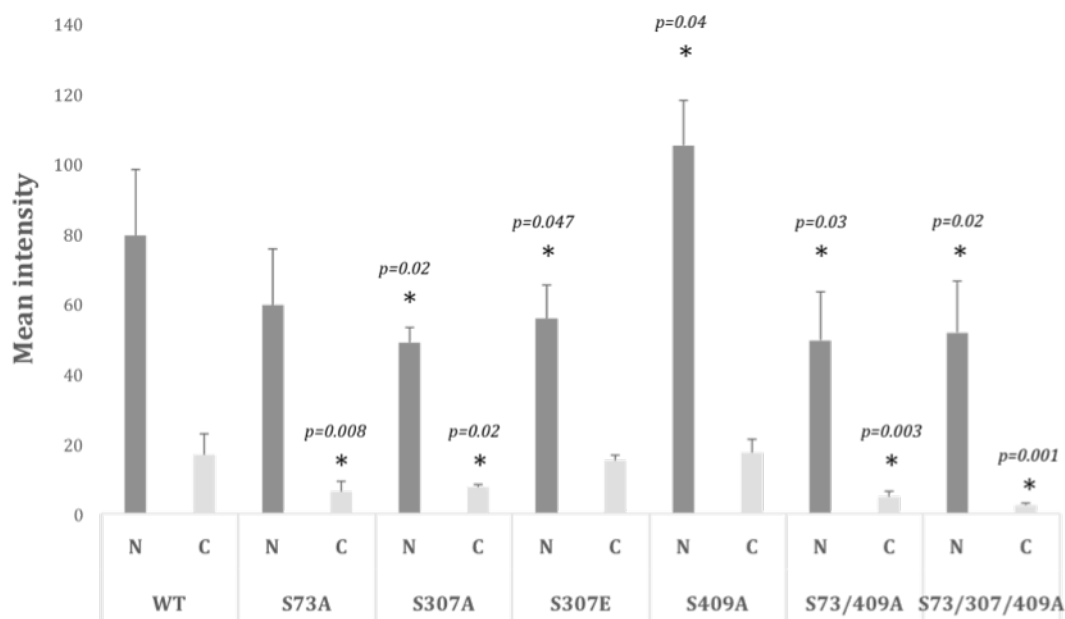
Figure 14: Bar graphs showing nuclear (N) and cytoplasmic (C) mean intensity levels of WT-MITF and various serine mutant constructs. *Student's t-tests were performed and p-values below 0.05 were considered statistically significant, n=22.*

	WT	S73A	S307A	S307E	S409A	S73/409A	S73/307/409A
C	17.40	9.47	13.35	21.29	14.16	8.82	4.42
N	82.60	90.53	86.65	78.71	85.84	91.18	95.58

Figure 15: Bar graphs showing nuclear and cytoplasmic mean intensities in percent. *The percentage in the nucleus varies from 79-96%.*

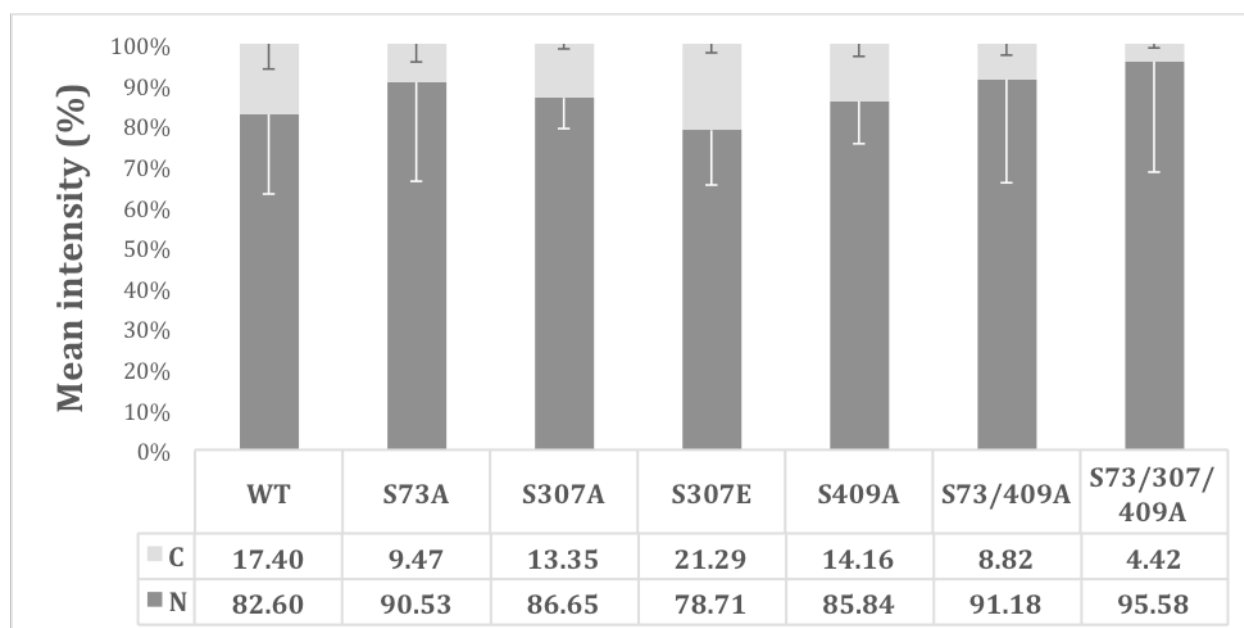Figures 14 and 15 show the quantifications of the nuclear and cytoplasmic mean intensities of the constructs. To determine the statistical significance, values of all serine mutants were compared to the wild type by using a Student's t-test. Figure 14 presents raw values and Figure 15 shows percentages of nuclear and cytoplasmic intensity levels.

The constructs S73A, S307A, S73/409A and S73/307A/409A showed a significant decrease in the intensity of cytoplasmic staining compared to the wild type. S307A, S307E, S73/409A and S73/307A/409A showed a significant decrease in the nuclear staining intensity, whereas S409A showed a significant increase in nuclear intensity when compared to the wild type.

4.2 Constructs having no effects on MITF localization, compaired to the wild type

Figures 16 and 17 show confocal images of constructs that did not have any significant effect on the subcellular localization of MITF compared to the wild type construct. These constructs, S100A, S298A, S384A, S397A, S298/307A/384A and S298/384A/397A all exhibit a similar staining pattern as the wild type: a strong nuclear and weak cytoplasmic signal.
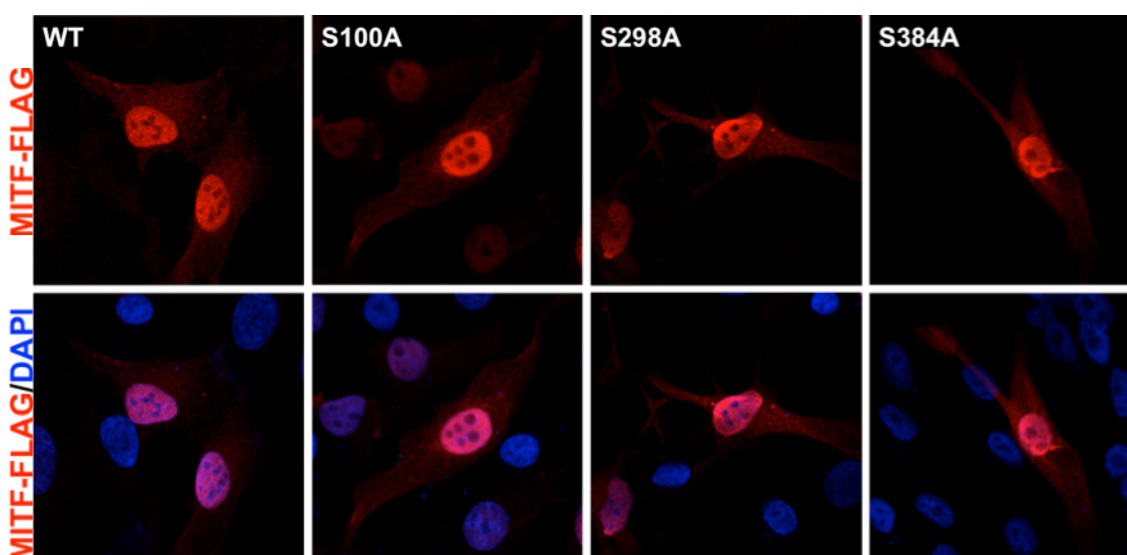
Figure 16: Mutant constructs showing no significant difference in mean intensity compared to the wild type.
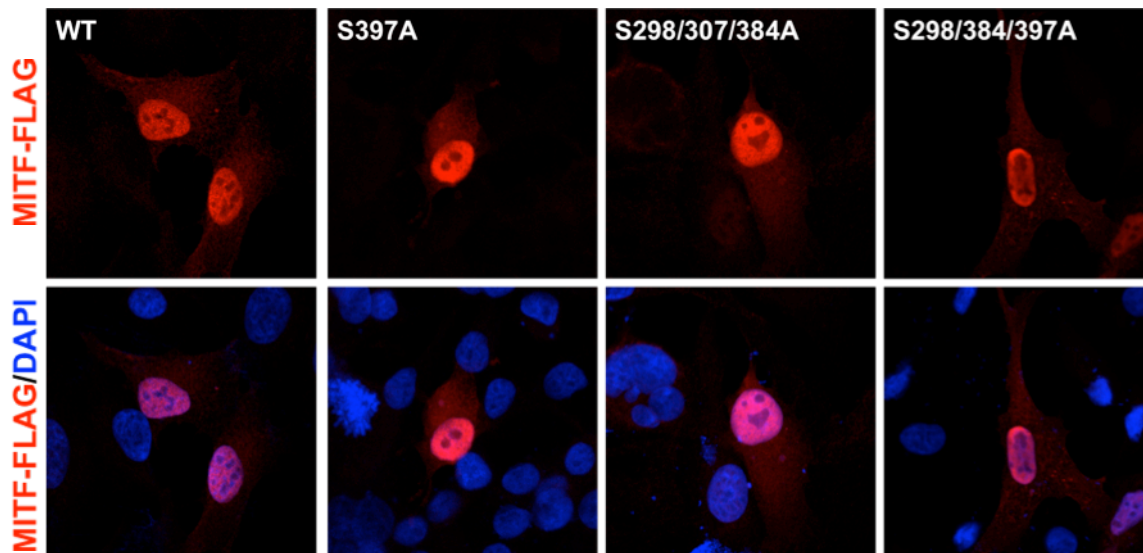
Figure 17: Mutant constructs showing no significant difference in mean intensity compared to the wild type.
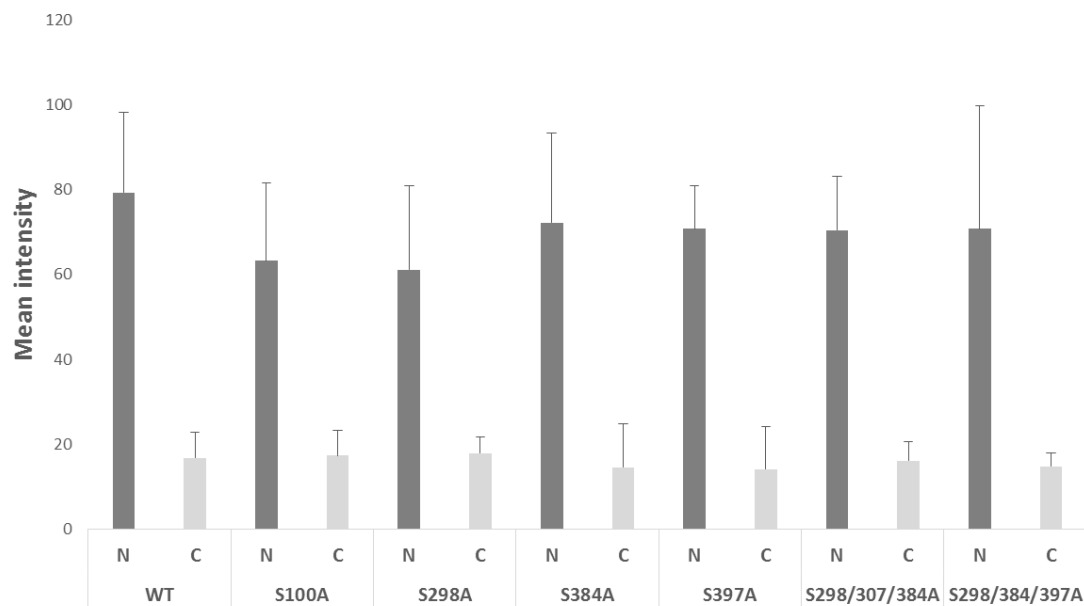
4.2.1 Mean intensity quantifications

Figure 18: Quantifications of nuclear and cytoplasmic mean intensities. *No significant difference in the subcellular localization of these constructs compared to the wild type was observed; n=22.*

	WT	S100A	S298A	S384A	S397A	S298/307 /384A	S298/384 /397A
C	17.40	21.45	22.57	16.77	16.58	18.58	17.19
N	82.60	78.55	77.43	83.23	83.42	81.42	82.81
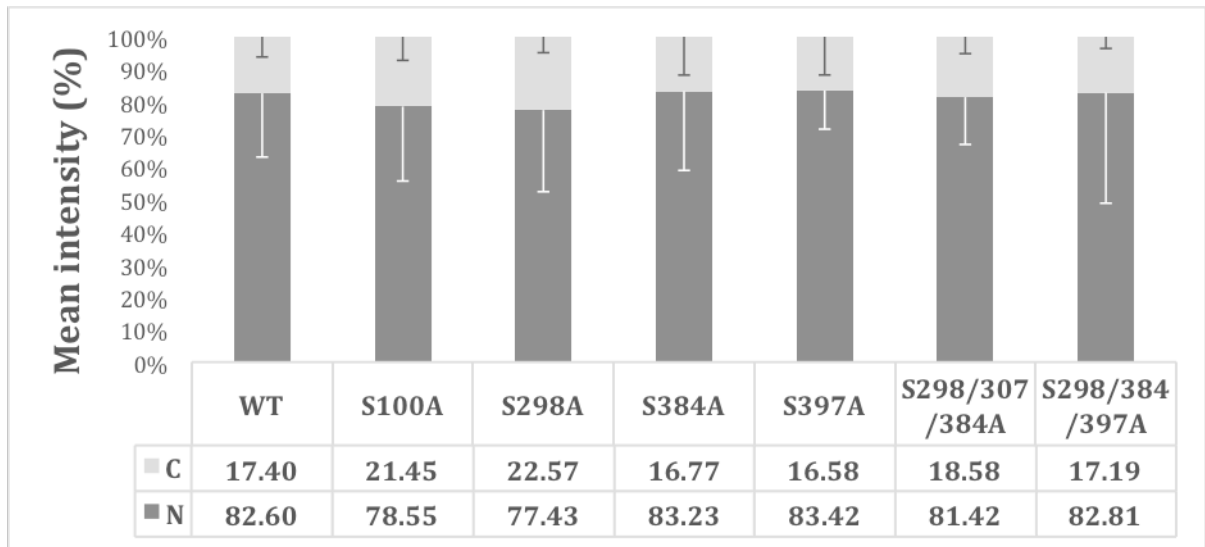
Figure 19: Representation of nuclear and cytoplasmic mean intensities in percent.

The mean intensity calculations for the constructs presented in Figures 16 and 17 are shown in Figures 18 and 19. Figure 18 shows the raw values of nuclear and cytoplasmic mean intensities and in Figure 19, results are shown in percent. No significant difference in the mean intensity for each of these constructs was observed when compared to the wild type. By looking at the percentages displayed in Figure 19, the mean intensity values of the nuclear stainings lie within a range of 77-83.5% for all of these constructs, which is not a significant difference according to Student's t-test.

5 Discussion

In this study we have shown that when the serine residues S73, S409 or S307 are phosphorylated, it significantly affects the subcellular localization of MITF. These serine sites might therefore play an important role in modulating MITF's function as transcriptional regulator in melanoma cells.

According to the results, mutation of S73 to alanine affects the subcellular localization of MITF in a way that it becomes significantly less cytoplasmic and almost all the protein is found within the nucleus. Since mutated S73 results in a decreased cytoplasmic fraction, phosphorylation of MITF at this residue might therefore be important for its cytoplasmic retention or stability. Alternatively, it may affect nuclear export. When the S73A mutant was present in a double or triple mutant construct (S73/409A and S73/307/409A), it had the same effect on MITF in terms of decreased cytoplasmic staining. Interestingly, the double and triple mutants showed weaker nuclear signals compared to the wild type construct. Similar to S73A, the S307A mutant showed a decrease in cytoplasmic staining intensity when compared to the wild type construct. In addition, it also showed significantly decreased MITF levels in the nucleus. This might explain why the S73/307/409A construct exhibited a decreased nuclear staining intensity. This difference in overall staining intensity may be due to different expression levels of the plasmid in the cells, or may reflect effects of the mutants on protein stability.

The most notable constructs were constructs S409A and S307E. S409A affected the localization of MITF by significantly increasing MITF levels in the nucleus. However, when S409A was combined in a double or triple mutant, it did not seem to increase the nuclear localization of MITF, rather decreasing it. This effect might have been caused by the other mutations present within these constructs. Transient transfections were used for these experiments, but that might lead to unequal expression levels of the constructs, the results must therefore be interpreted with caution. Generation of stable cell lines might lead to a better understanding of the effects S409 has on the nuclear localization of MITF. Stability of the mutant constructs should also be investigated in the future.

S307E is supposed to mimic the phosphorylated state of the particular amino acid but intriguingly there was a significant decrease in the nuclear localization of MITF, similar to the S307A construct. With a p-value of 0.047, more repeats might be required in order to draw definite conclusions. However, in contrast to S307A, the S307E mutant does not seem to have an effect on the cytoplasmic fraction of MITF when compared to the wild type. Further research has to be conducted in order to evaluate why these two constructs behave this way.

The rest of the serine mutants analyzed in this study did not show an effect on the subcellular localization of MITF. Even though these constructs might not influence MITF's localization, they might exhibit other effects on MITF such as changes in its transcriptional activity, protein interactions or stability.

In conclusion, when S73 in MITF is phosphorylated, presumably by ERK downstream of hyperactive BRAF, its cytoplasmic fraction might increase or at least become stabilized. It would be of interest to generate a S73E mutant, mimicking the phosphorylated state of MITF at this residue, to assess this further. When S307, S73/409 and S73/307/409 are phosphorylated, an increased amount of MITF is present in the nucleus, suggesting that those sites, when phosphorylated, enhance MITF's transcriptional activity. S409, when phosphorylated, seems to affect MITF's stability, which is in agreement with the literature. The same might apply to S73 as it seems that when phosphorylated it affects MITF's transcriptional activity (Wu et al., 2000).

References

Alberts, Johnson, Lewis, Morgan, Raff, Roberts, Walter. (2015). Molecular Biology of the Cell. Abingdon, New York: Garland Science.

Bondurand, N., et al. (2000). "Interaction among SOX10, PAX3 and MITF, three genes altered in Waardenburg syndrome." Hum Mol Genet 9(13): 1907-1917.

Bowerman, B. (2008). "Cell signaling. Wnt moves beyond the canon." Science 320(5874): 327-328.

Cichorek, M., et al. (2013). "Skin melanocytes: biology and development." Postepy Dermatol Alergol 30(1): 30-41.

Delghandi, M. P., et al. (2005). "The cAMP signalling pathway activates CREB through PKA, p38 and MSK1 in NIH 3T3 cells." Cell Signal 17(11): 1343-1351.

Landlæknisembættið. Hollráð: Sortuæxli. Sótt 18. maí 2016 af http://www.hudlaeknastodin.is/page31/page39/page39.html

Lee, M., et al. (2000). "Direct regulation of the Microphthalmia promoter by Sox10 links Waardenburg-Shah syndrome (WS4)-associated hypopigmentation and deafness to WS2." J Biol Chem 275(48): 37978-37983.

Mansky, K. C., et al. (2002). "Microphthalmia transcription factor is a target of the p38 MAPK pathway in response to receptor activator of NF-kappa B ligand signaling." J Biol Chem 277(13): 11077-11083.

Morrison, D. K. (2012). "MAP kinase pathways." Cold Spring Harb Perspect Biol 4(11).

Overview of Post-Translational Modifications. (Year unknown). Sótt 18. maí 2016 af https://www.thermofisher.com/is/en/home/life-science/protein-biology/protein-biology-learning-center/protein-biology-resource-library/pierce-protein-methods/overview-post-translational-modification.html

Phosphorylation. (Year unknown). Sótt 18. maí 2016 af https://www.thermofisher.com/is/en/home/life-science/protein-biology/protein-biology-learning-center/protein-biology-resource-library/pierce-protein-methods/phosphorylation.html

Ploper, D., et al. (2015). "MITF drives endolysosomal biogenesis and potentiates Wnt signaling in melanoma cells." Proc Natl Acad Sci U S A 112(5): E420-429.

Pogenberg, V., et al. (2012). "Restricted leucine zipper dimerization and specificity of DNA recognition of the melanocyte master regulator MITF." Genes Dev 26(23): 2647-2658.

Potterf, S. B., et al. (2000). "Transcription factor hierarchy in Waardenburg syndrome: regulation of MITF expression by SOX10 and PAX3." Hum Genet 107(1): 1-6.

Price, E. R., et al. (1998). "Lineage-specific signaling in melanocytes. C-kit stimulation recruits p300/CBP to microphthalmia." J Biol Chem 273(29): 17983-17986.

Raker, V. K., et al. (2016). "The cAMP Pathway as Therapeutic Target in Autoimmune and Inflammatory Diseases." Front Immunol 7: 123.

Rao, T. P. and M. Kuhl (2010). "An updated overview on Wnt signaling pathways: a prelude for more." Circ Res 106(12): 1798-1806.

Shain, A. H. and B. C. Bastian (2016). "From melanocytes to melanomas." Nat Rev Cancer. 1-14

Verastegui, C., et al. (2000). "Regulation of the microphthalmia-associated transcription factor gene by the Waardenburg syndrome type 4 gene, SOX10." J Biol Chem 275(40): 30757-30760.

Wellbrock, C. and I. Arozarena (2015). "Microphthalmia-associated transcription factor in melanoma development and MAP-kinase pathway targeted therapy." Pigment Cell Melanoma Res 28(4): 390-406.

Wu, M., et al. (2000). "c-Kit triggers dual phosphorylations, which couple activation and degradation of the essential melanocyte factor Mi." Genes Dev 14(3): 301-312.